EFDA–JET–CP(14)01/29

A. Drenik, M. Oberkofler, D. Alegre, U. Kruezi, S. Brezinsek,
M. Mozetič, I. Nunes, M. Wischmeier, C. Giroud, G. Maddison,
C. Reux and JET EFDA contributors

Mass Spectrometry Analysis of Impurity Seeded Discharges in JET-ILW

“This document is intended for publication in the open literature. It is made available on the understanding that it may not be further circulated and extracts or references may not be published prior to publication of the original when applicable, or without the consent of the Publications Officer, EFDA, Culham Science Centre, Abingdon, Oxon, OX14 3DB, UK.”

“Enquiries about Copyright and reproduction should be addressed to the Publications Officer, EFDA, Culham Science Centre, Abingdon, Oxon, OX14 3DB, UK.”

The contents of this preprint and all other JET EFDA Preprints and Conference Papers are available to view online free at www.iop.org/Jet. This site has full search facilities and e-mail alert options. The diagrams contained within the PDFs on this site are hyperlinked from the year 1996 onwards.

Mass Spectrometry Analysis of Impurity Seeded Discharges in JET-ILW

A. Drenik[1], M. Oberkofler[2], D. Alegre[3], U. Kruezi[4], S. Brezinsek[5], M. Mozetič[1], I. Nunes[6], M. Wischmeier[2], C. Giroud[4], G. Maddison[4], C. Reux[7] and JET EFDA contributors*

JET-EFDA, Culham Science Centre, OX14 3DB, Abingdon, UK

[1]Jožef Stefan Institute, EURATOM Association Jamova 39, 1000 Ljubljana, Slovenia
[2]Max-Planck-Institut für Plasmaphysik, Boltzmannstraße 2, D-85748 Garching, GermanyMax
[3]As. EURATOM-CIEMAT, Av. Complutense 40, 28040 Madrid, Spain,
[4]Culham Centre for Fusion Energy, Abingdon, Oxon, OX14 3DB, United Kingdom
[5]IEF - Plasmaphysik FZ Jülich, EURATOM Association, 52425 Jülich, Germany
[6]Associação EURATOM - IST, Instituto de Plasmas e Fusão Nuclear, 1049 - 001, Lisboa, Portugal
[7]CEA, IRFM, EURATOM Assoc, F-13108 St Paul Les Durance, France
** See annex of F. Romanelli et al, "Overview of JET Results", (24th IAEA Fusion Energy Conference, San Diego, USA (2012)).*

Preprint of Paper to be submitted for publication in Proceedings of the
21st International Conference on Plasma Surface Interactions, Kanazawa, Japan
26th May 2014 – 30th May 2014

ABSTRACT

Presented are the results of the first mass spectrometry study of impurities at JET with the ILW. Measurements are performed with the newly-installed RGA system that allows for data acquisition in all stages of machine operation. Impurities are found in the 16 – 20AMU range, at 28AMU (N_2) and 40AMU (Ar). The main contaminants are water and nitrogen, which are present only in low amounts. During seeded discharges, the impurity content increases, however it falls back to non-seeded quantities in subsequent non-seeded discharges, exhibiting only slight legacy levels.

1. INTRODUCTION

Since the installation of the ITER-like wall (ILW), JET provides a unique test bed to study plasma operation in the ITER material mix: Be plasma-facing components (PFCs) in the main chamber and W components in the divertor (1). W sputtering which determines the lifetime of the divertor components in the Be/W mix is induced by intrinsic impurities such as Be, O and C, and extrinsic impurities like N_2 and Ar(2), though the C and Be content are orders of magnitude lower in quantity in comparison with the carbon wall(3). As the JET-ILW does not include carbon-based PFCs, nitrogen is being seeded to replace carbon as the radiating species in the plasma edge and mitigate heat loads at the W target plates(4). Argon is routinely used as gas for the disruption mitigation system in JET which injects massive amounts of Ar + D_2 mixture to reduce or prevent damage to PFCs caused by disruptions(5). Therefore, a complex set of impurities can interact with the first wall and impact the plasma operation, and identification and quantification of these species and their temporal evolution as legacy gas is of interest.

In this paper, we present a residual gas analysis (RGA) study of the impurity content during impurity seeded discharges at JET. Residual gas analysis relies on the use of mass spectrometers (MS), placed typically downstream of the plasma volume in pump ducts. As the transmission path from the plasma to the MS is long, charges particles, metastable species and neutral non-noble atoms do not reach the MS, and only the content of inert species (stable molecules and noble gases) can be analysed. However, unlike other diagnostic techniques that do not suffer from such limitations (such as VUV spectroscopy), the detection by MS provides information on the impurity content throughout all stages of the tokamak operation (discharge phase, outgassing after a disruption, time between discharges …). This contribution is the first report based on RGA measurements with both sufficient temporal resolution to monitor trends in the discharge phase, as well as continuous recording between discharges.

2. EXPERIMENTAL

The impurity content of the tokamak vacuum vessel was analysed with a newly installed sub-divertor residual gas analysis system(6). It is based on a Hiden Analytical HAL 201 RC mass spectrometer (MS), located in the sub-divertor. The spectrometer is placed inside a soft iron chamber for magnetic shielding, which enables accurate measurements in all stages of the discharge. The pressure in the

sub-divertor reaches up to 10^{-3} mbar during normal discharges, which exceeds the operational range of the MS. In order to allow RGA operation during discharges, the MS is differentially pumped and connected to the main volume of the sub-divertor diagnostic system through a tuneable gas flow restrictor. In the measurements presented in this paper, the flow restrictor was set to reduce the pressure in the RGA chamber by approximately a factor of 10.

In the discharge phase, the RGA was measuring intensities at discrete masses with the sampling time of 1.4 s which allowed for recording of several data points in the discharge flattop phase of about ten seconds. In most cases, the intensities at the following discrete mass to charge ratios were recorded: 2, 3, 4, 12, 13, 14, 15, 16, 17, 18, 19, 20, 21, 23, 28, 29, 30, 31, 32 and 40AMU/e. This set of masses was selected primarily for the purpose of N_2 seeded experiments. The 2 – 4AMU range is expected to be populated by hydrogen species, the 15 – 21AMU range is expected to be populated by ammonia, water and methane in all possible isotope configurations. Mass 28AMU is expected to be populated primarily by N_2, but also by CO. Mass 30AMU is attributed to $_{15}N_2$, mass 32AMU to O_2, mass 40AMU to Ar and mass 44 to CO_2. Mass 23AMU was recorded as a reference "zero signal". Since we expect no molecules or noble gases to contribute to the signal at 23AMU, it is used for estimation of the noise level.

In between the discharges, full spectra were acquired in the 1 – 45AMU range with the resolution of 0.1AMU and the sampling time of 23 s. As the RGA system has not yet been calibrated, the intensities cannot be linked to absolute abundances of the detected species, however the ability to acquire data during all phases of the discharge allows for uninterrupted monitoring of the trends in the sub-divertor gas composition. The vast majority of the data used in this study is obtained from discharges between JET Pulse Numbers: 85356 and 85462. This data set consists of uninterrupted RGA recordings of non-seeded sessions (JET Pulse Numbers: 85356 – 85404), five consecutive nitrogen seeding sessions in which a total of 16.7 barl nitrogen was injected (JET Pulse Numbers: 85405 – 85436) and a session with deliberate argon injections (JET Pulse Numbers: 85445 – 85457, 59.9 barl). This provides the opportunity to characterize the sub-divertor gas composition in un-seeded discharges, study the direct impact of seeding and its long-term legacy effects.

3. RESULTS AND DISCUSSION

The analogue spectra shown in Figure 1 were recorded between discharges, before the start of the next discharge. The impurity content is dominated by N_2, followed by water and CO_2. Trace amounts of O_2 are also detected. The strongest peak in the 15 – 20AMU range is at 18AMU, followed by 19 and 17AMU. This indicates a low D/(D+H) ratio (however, not pure H composition). As methane is the only candidate molecule that could contribute to mass 15AMU, the absence of a peak at 15AMU suggests that is present only in negligible amounts. The hydrogen content varies with the tokamak operation. In the morning before the start of experiments, it exhibits a low D/(D+H) ratio. Since plasmas are ignited in deuterium, not hydrogen, the high hydrogen content in the spectra is most likely explained by a water leak near the location of the MS(7). In the course of the experimental

session, the hydrogen range, as well as the whole spectrum, is dominated by D_2. The morning spectra are thus the best indicator of the intrinsic gas composition at the location of the MS. While the rest of the spectral features are not constant, their variations do not exhibit the same trend as 4AMU, suggesting that the influx of impurities from the main chamber to the sub-divertor in non-seeded discharges is not large enough to influence the atmosphere at the location of the MS.

To discuss the amounts of impurities recorded during the discharge phase, instead of intensities, we observe their shot integrals, i.e. integral of the recording at a specific intensity throughout the duration of the discharge phase(8). At mass 23AMU (the "zero signal"), the average shot density is $3.2 \cdot 10^{-9}$, while the standard deviation is $6.3 \cdot 10^{-8}$. Shot integrals of species of detectable densities thus begin above 10^{-7}.

During most dry runs – injections of gas without plasma operation – the quantity of injected D_2 is of the order of 0.01 barl, and a response in the RGA recordings is observed only at 4AMU. However, at a dry run (JET Pulse Number: 85226) in which the quantity of injected D_2 is comparable to the quantity injected during discharges (2.57 barl), a slight response can be observed also at 20AMU ($3.3 \cdot 10^{-6}$), 18 ($1.7 \cdot 10^{-6}$) and 19AMU ($1.9 \cdot 10^{-6}$), and 28AMU ($9.2 \cdot 10^{-7}$), indicating partially deuterated water and nitrogen. This could be attributed to desorption of water from the gas lines through which the D_2 is flowing. The dominance of mass 20AMU indicates a high D/(D+H) ratio, which could be explained by isotope exchange of water molecules in the predominantly D_2 atmosphere.

Compared to (large D_2 quantity) dry runs, the amount of impurities recorded during non-seeded discharges increases considerably. The most abundant impurity is deuterated water at 18 and 20AMU where the shot integrals increase by a factor of 5, while the shot integrals at 19AMU remains at the dry run values. The low intensity at 19AMU indicates a higher D/(D+H) ratio than during the dry run. Other detected impurities are N_2 and O_2, and trace amounts of Ar. The average shot integrals values in non-seeded discharges are listed in Table 1. The increased impurity content is expected as plasma operation introduces new mechanisms of impurity production (thermal desorption, physical sputtering and surface reactions between reactive species).

In nitrogen seeded discharges (JET Pulse Numbers: 85405 – 85436), the impurity content is dominated by mass 28AMU. The shot integral values depend on the quantity of the seeded gas, however they are at least an order of magnitude higher than in non-seeded discharges (Fig 1, top). The signal at 28AMU responds to the seeding with an average delay of 2.5 seconds and decays with the average time of 4 seconds after the end of the discharge. Along with the increase at 28AMU, nitrogen seeding gives rise to the intensities in the 16 – 20AMU range (Figure 2, top), especially at 17 and 18AMU, which could be explained by conversion of nitrogen into ammonia. The heaviest seeding (2.58 barl) occurs at discharge JET Pulse Number: 85425, where the shot integral at mass 28AMU is $1.5 \cdot 10^{-4}$, at 16AMU $1.1 \cdot 10^{-5}$, at 17AMU $2.4 \cdot 10^{-5}$, at 18AMU $2.8 \cdot 10^{-5}$, at 19AMU $1.1 \cdot 10^{-5}$, and at 20AMU $1.0 \cdot 10^{-5}$. The relatively high intensities of lower masses suggest that D/(D+H) ratio of the produced ammonia is relatively low which, in turn, indicates different isotope exchange mechanisms for water and ammonia.

During the nitrogen seeding sessions, several isolated non-seeded discharges occur. During those, the shot integrals at 28AMU, as well as in the 16 – 19AMU range are slightly above average, as listed in Table 2. While there is no strong correlation to the amount of seeded nitrogen prior to the non-seeded discharge, the highest values of the shot integrals do occur after the largest amount of injected nitrogen.

The intensity at 28AMU and the 16 – 19AMU in the post-discharge analogue recordings gradually increases through the course of the seeding sessions (Figure 1 and 2, bottom), indicating a slight level of nitrogen retention at the location of the MS. The usual time between discharges is around 30 minutes which is frequent enough for the nitrogen population to build up. The intensity drops before the end of the seeding session, namely between discharges JET Pulse Numbers: 85434 and 85435 which are almost three hours apart. During that time, nitrogen (and ammonia) content is reduced to almost non-seeded values.

After the seeding session, the shot integral at 28AMU is twice the average value and decays to the average value in the following 6 discharges. Similar behaviour is observed in the 16 – 19AMU range. The non-seeded session is followed by a session of deliberate Ar injection (JET Pulse Numbers: 85445 – 85457). In the course of this session, shot integral values at 28AMU, as well as 16, 17 and 18AMU continue to decay steadily, reaching values below the average. The average values are reached in the subsequent operator session. Shot integrals of mass 19AMU decay only during the first 6 discharges, and remain at constant values (around the average non-seeded value) during the Ar injection session, suggesting that in this session, the water content is not reduced as strongly as the content of nitrogen species.

Argon contamination mostly occurs in the scope of the operation of the disruption mitigation valve (DMV), where a substantial amount of an argon-containing gas mixture (up to 36 barl 90 vol. % D_2 +10 vol. %Ar) is injected into the reactor vessel. This causes a rapid increase of the pressure (up to $2 \cdot 10^{-2}$ mbar) and extinguishes the plasma(5a). This routine control tool is used for all plasma discharges above 2.5T. The injection of the DMV gas is reflected in the RGA recording as a sharp increase at the masses 40 (Ar^{+}) and 20AMU (Ar^{++}). The response and decay times are very similar in comparison with nitrogen seeding. Typically, between 9 and 10 barl of the disruption mitigation was injected, resulting in shot integrals with the average value of $(1.2 \pm 0.6) \cdot 10^{-4}$ for 40AMU and $(4.9 \pm 2.1) \cdot 10^{-5}$ for 20AMU.

As Ar is injected as means of preventing disruptions, there is no clearly separated region of discharges with and without argon injection. The only session of deliberate Ar injection (discharges JET Pulse Numbers: 85445 – 85457) in which 59.9 barl of Ar was injected is not followed by normal tokamak operation, which doesn't allow for a study of long term legacy as in the case of nitrogen. Instead, we observe the behaviour of Ar content in the discharges following a discharge with Ar injection. The average value of the shot integral at 40AMU in the first discharge after Ar injection is $(6.8 \pm 2.7) \cdot 10^{-7}$. Shot integral values of subsequent discharges, normalised to the first discharge after Ar injections are shown in Figure 3. After the first shot, the value remains constant, at about

60 % of the first shot value. During normal DMV operation, the post-discharge spectra show no sign of Ar legacy, however a slight increase is observed during the Ar injection session.

4. CONCLUSIONS

The MS measurements indicate low impurity content in JET with the ILW, both in the atmosphere between discharges, as well as during the non-seeded discharges, where the main contaminants are water and nitrogen. In contrast with the carbon wall(9), no CH_x species are detected. The dry run recordings reveal that a possible source of impurities is desorption from the gas lines through which D_2 is passed.

The presence of impurities increases significantly during seeding. Nitrogen seeding gives rise to increase of intensities in the 16 – 20AMU range in the spectra, beside the 28AMU peak attributed to N_2, indicating at conversion of N_2 to NH_3. The presence of impurities decreases significantly after the termination of seeding, however a decay spanning over 6 discharges is observed before it is completely reduced to average non-seeded values. The further decay over the next 12 discharges is most likely linked to the specifics of heavy Ar injection. In contrast to operation with the carbon wall, the present levels of nitrogen legacy have only a marginal impact on plasma operation.
During normal DMV operation, a slight Ar legacy is observed only in the first discharge after the disruption-mitigated discharge, however more dedicated studies are required to determine the long-term legacy.

ACKNOWLEDGEMENT

This work was supported by EURATOM and carried out within the framework of the European Fusion Development Agreement. The views and opinions expressed herein do not necessarily reflect those of the European Commission.

REFERENCES

[1]. (a) Horton, L.; Contributors, E.-J., Fusion Engineering and Design 2013, **88** (6–8), 434–439; (b) Romanelli, F.; Contributors, J. E., Nuclear Fusion 2013, 53 (10).

[2]. Neu, R. L.; Brezinsek, S.; Beurskens, M.; Bobkov, V.; de Vries, P.; Giroud, C.; Joffrin, E.; Kallenbach, A.; Matthews, G. F.; Mayoral, M. L.; Pautasso, G.; Putterich, T.; Ryter, F.; Schweinzer, J.; Team, A. U.; Contributors, J. E., IEEE Transactions on Plasma Science 2014, **42** (3), 552–562.

[3]. Brezinsek, S.; Jachmich, S.; Stamp, M. F.; Meigs, A. G.; Coenen, J. W.; Krieger, K.; Giroud, C.; Groth, M.; Philipps, V.; Grunhagen, S.; Smith, R.; van Rooij, G. J.; Ivanova, D.; Matthews, G. F.; Contributors, J.-E., Journal of Nuclear Materials 2013, **438**, S303–S308.

[4]. Giroud, C.; Maddison, G. P.; Jachmich, S.; Rimini, F.; Beurskens, M. N. A.; Balboa, I.; Brezinsek, S.; Coelho, R.; Coenen, J. W.; Frassinetti, L.; Joffrin, E.; Oberkofler, M.; Lehnen, M.; Liu, Y.; Marsen, S.; McCormick, K.; Meigs, A.; Neu, R.; Sieglin, B.; van Rooij, G.; Arnoux,

G.; Belo, P.; Brix, M.; Clever, M.; Coffey, I.; Devaux, S.; Douai, D.; Eich, T.; Flanagan, J.; Grunhagen, S.; Huber, A.; Kempenaars, M.; Kruezi, U.; Lawson, K.; Lomas, P.; Lowry, C.; Nunes, I.; Sirinnelli, A.; Sips, A. C. C.; Stamp, M.; Wiesen, S.; Contributors, J.-E., Nuclear Fusion 2013, **53** (11).

[5]. (a) Lehnen, M.; Alonso, A.; Arnoux, G.; Baumgarten, N.; Bozhenkov, S. A.; Brezinsek, S.; Brix, M.; Eich, T.; Gerasimov, S. N.; Huber, A.; Jachmich, S.; Kruezi, U.; Morgan, P. D.; Plyusnin, V. V.; Reux, C.; Riccardo, V.; Sergienko, G.; Stamp, M. F.; Contributors, J. E., Nuclear Fusion 2011, 51 (12); (b) Lehnen, M.; Arnoux, G.; Hartmann, N.; Brezinsek, S.; Devaux, S.; Huber, A.; Jachmich, S.; Kruezi, U.; Matthews, G. F.; Reux, C.; Riccardo, V.; Sieglin, B.; Stamp, M. F.; de Vries, P. C.; Contributors, J. E., Journal of Nuclear Materials 2013, **438**, S102–S107.

[6]. Kruezi, U.; Sergienko, G.; Morgan, P. D.; Matthews, G. F.; Brezinsek, S.; Vartanian, S.; Contributors, J.-E., Review of Scientific Instruments 2012, **83** (10).

[7]. Douai, D.; Brezinsek, S.; Esser, H. G.; Joffrin, E.; Keenan, T.; Knipe, S.; Kogut, D.; Lomas, P. J.; Marsen, S.; Nunes, I.; Philipps, V.; Pitts, R. A.; Shimada, M.; de Vries, P.; Contributors, J. E., Journal of Nuclear Materials 2013, **438**, S1172–S1176.

[8]. Oberkofler, M.; Douai, D.; Brezinsek, S.; Coenen, J. W.; Dittmar, T.; Drenik, A.; Romanelli, S. G.; Joffrin, E.; McCormick, K.; Brix, M.; Calabro, G.; Clever, M.; Giroud, C.; Kruezi, U.; Lawson, K.; Linsmeier, C.; Martin Rojo, A.; Meigs, A.; Marsen, S.; Neu, R.; Reinelt, M.; Sieglin, B.; Sips, G.; Stamp, M.; Tabares, F. L., Journal of Nuclear Materials 2013, (0).

[9]. Brezinsek, S.; Loarer, T.; Krieger, K.; Jachmich, S.; Tsalas, M.; Coffey, I.; Esser, H. G.; Eich, T.; Fundamenski, W.; Giroud, C.; Gruenhagen, S.; Huber, A.; Kruezi, U.; Knipe, S.; Maddison, G. P.; McCormick, K.; Meigs, A. G.; Morgan, P.; Philipps, V.; Sergienko, G.; Stagg, R.; Stamp, M. F.; Tabares, F. L.; Contributors, J. E., Nuclear Fusion 2011, **51** (7).

Mass [AMU]	Average shot integral [a.u.]
4	$(5.8\pm2.2)\cdot10^{-5}$
16	$(8.5\pm3.2)\cdot10^{-7}$
17	$(8.9\pm5.9)\cdot10^{-7}$
18	$(8.7\pm3.1)\cdot10^{-6}$
19	$(2.5\pm1.6)\cdot10^{-6}$
28	$(6.5\pm3.4)\cdot10^{-6}$
32	$(1.9\pm0.8)\cdot10^{-6}$

Table 1: Average shot integrals in non-seeded discharges (JET Pulse Numbers: 85359 – 85404) at impurity-related intensities. Masses 20 and 40AMU are omitted as they are dominated by Ar from frequent disruption-mitigation gas injections.

	shot integral [a.u.]					Injected N_2
JPN	16 AMU	17 AMU	18 AMU	19 AMU	28 AMU	[barl]
85415	$1.21\cdot10^{-6}$	$1.92\cdot10^{-6}$	$8.17\cdot10^{-6}$	$2.34\cdot10^{-6}$	$1.1\cdot10^{-5}$	4.03
85421	$1.30\cdot10^{-6}$	$1.74\cdot10^{-6}$	$1.2\cdot10^{-5}$	$3.93\cdot10^{-6}$	$1.5\cdot10^{-5}$	1.5
85424	$1.38\cdot10^{-6}$	$1.93\cdot10^{-6}$	$7.81\cdot10^{-6}$	$1.89\cdot10^{-6}$	$1.1\cdot10^{-5}$	2.3
85432	$2.05\cdot10^{-6}$	$3.59\cdot10^{-6}$	$1.1\cdot10^{-5}$	$3.03\cdot10^{-6}$	$1.6\cdot10^{-5}$	7.17
85435	$1.06\cdot10^{-6}$	$2.23\cdot10^{-6}$	$8.10\cdot10^{-6}$	$3.26\cdot10^{-6}$	$1.0\cdot10^{-5}$	1.35
85438	$1.35\cdot10^{-6}$	$2.19\cdot10^{-6}$	$8.65\cdot10^{-6}$	$3.43\cdot10^{-6}$	$1.2\cdot10^{-5}$	0.55

Table 2: Shot integral values in non-seeded discharges during nitrogen seeding sessions, and amount of nitrogen seeded prior to the non-seeded discharge.

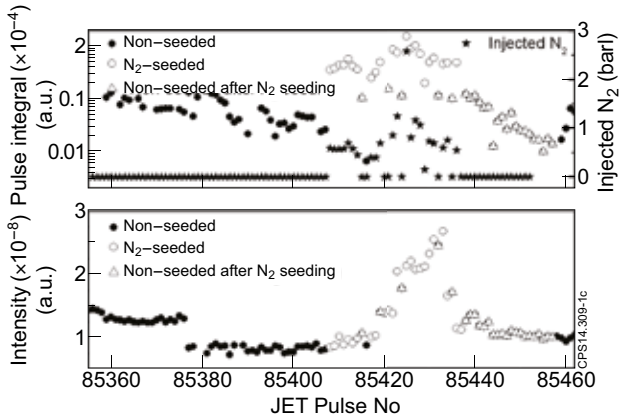

Figure 1: Shot integrals at 28AMU and quantities of seeded N_2 (top) and post-discharge recording intensities (bottom) at 28AMU.

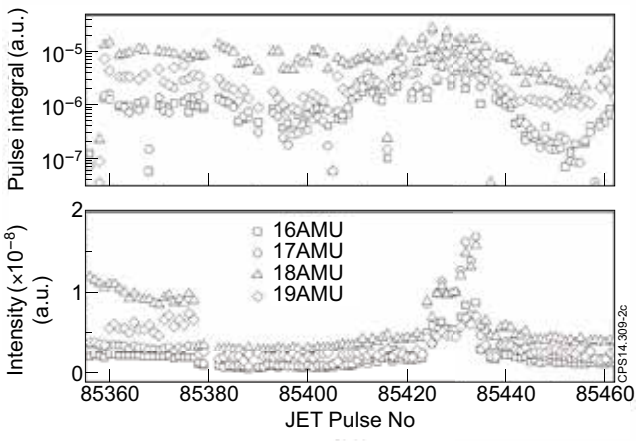

Figure 2: Shot integrals at (top) and post-discharge recording intensities (bottom) in the 16 – 19AMU range.

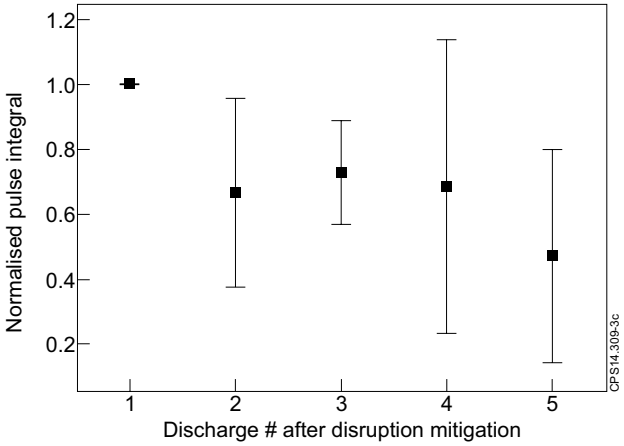

Figure 3: Relative shot integrals at 40AMU in discharges following a disrupted discharge – the integrals are normalised to the first discharge after the disruption.